

# ALMA MEMO 573

## Limits on Phase Correction Performance Due to Differences Between Astronomical and Water-Vapour Radiometer Beams

B. Nikolic, R. E. Hills and J. S. Richer

*Mullard Radio Astronomy Observatory, Cavendish Laboratory, Cambridge CB3 0HE, UK*

16 November 2007

### ABSTRACT

Using high-resolution three-dimensional realisations of turbulent fields, we investigate the limits on achievable performance of atmospheric phase correction using water-vapour radiometers arising from following effects: the incoherent measurement of power from water by the radiometers (in contrast to coherent detection of the astronomical signal); the different tapers of the response patterns of the astronomical and radiometer receivers; and, the differences in the directions of the radiometer and astronomical beams. We quantify the limit on performance as the fraction of atmospheric phase fluctuations that is not tracked by the radiometers. We find that, for parameters relevant for ALMA, the performance in high-frequency bands will be limited in approximately equal parts by the two effects, i.e., the differences due the incoherent vs coherent processes measured by the two receivers, together with their different tapers, and the angular displacements of the beams. For the lower frequency bands, the angular displacements of the beams becomes the dominant source of error.

### 1 INTRODUCTION

The ALMA project will use 183 GHz water-vapour radiometers (WVRs) to measure the fluctuations in atmospheric properties along the line of sight of each of the 12m telescopes in the array. These measurements by the WVRs, together with ancillary data collected by other instruments, will be used to infer corrections for the phase fluctuations in the astronomical signal introduced by the atmosphere.

The goal of this note is to investigate how the following effects limit the accuracy with which this phase corrections may be done:

- (i) The fact that the WVRs measure the power of emission from water while the phase fluctuation are a results of excess path due to water vapour within the coherent astronomical beam;
- (ii) The different illuminations patterns on the primary reflector of the WVR and astronomical beams; and,
- (iii) The angular offsets between the astronomical and WVR beams.

In order not to obscure the above effects we do not consider the effect of measurement error within the WVRs or the uncertainties associated with converting these measurements to excess path lengths.

This topic has been investigated before by Gibb & Harris (2000). This note extends on their work by:

- (i) Using high-resolution three-dimensional simulations of turbulence to quantify the difference between fluctuations of the phase of the astronomical signal and the radiometer outputs.
- (ii) Directly computing the beams rather than assuming they are Gaussian.
- (iii) Taking into account the coherent nature of the astronomical signal.

The ALMA Memo by Asaki et al. (2005) also uses statistical realisations of turbulence to simulate phase fluctuations, although their aim is to investigate phase correction for the ALMA Compact Array. We note that our method differs in that we directly simulate the three dimensional turbulence and compute the effect on the astronomical and WVR signals while they simulate two dimensional screens with varying structure functions.

### 2 METHOD

We want to calculate how the phase of an astronomical is affected by the turbulence and how well the WVRs can trace and predict these fluctuations. There are three main stages to this:

- (i) Generating high resolution, three dimensional, realisations of turbulent fields
- (ii) Calculating the astronomical and WVR beam shapes as functions of height
- (iii) Using the above two items to generate time series of phase of the astronomical signal and WVR measurements.

In this note we assume that fluctuations of atmospheric properties are sufficiently described by only a single variable,  $q(x, y, z)$ , which represents the water vapour content. To simplify calculations we assume that  $q$  describes variation about the mean so that  $\langle q \rangle = 0$ .

We next describe how  $q$  influences the propagation of astronomical radiation and the what the WVRs measure. We make the following assumptions:

- (i) That fluctuation in refractive index of the atmosphere are directly proportional to  $q$  so that  $n(x, y, z) - 1 \propto q(x, y, z)$ .
- (ii) That emission at frequencies that the WVRs measure from

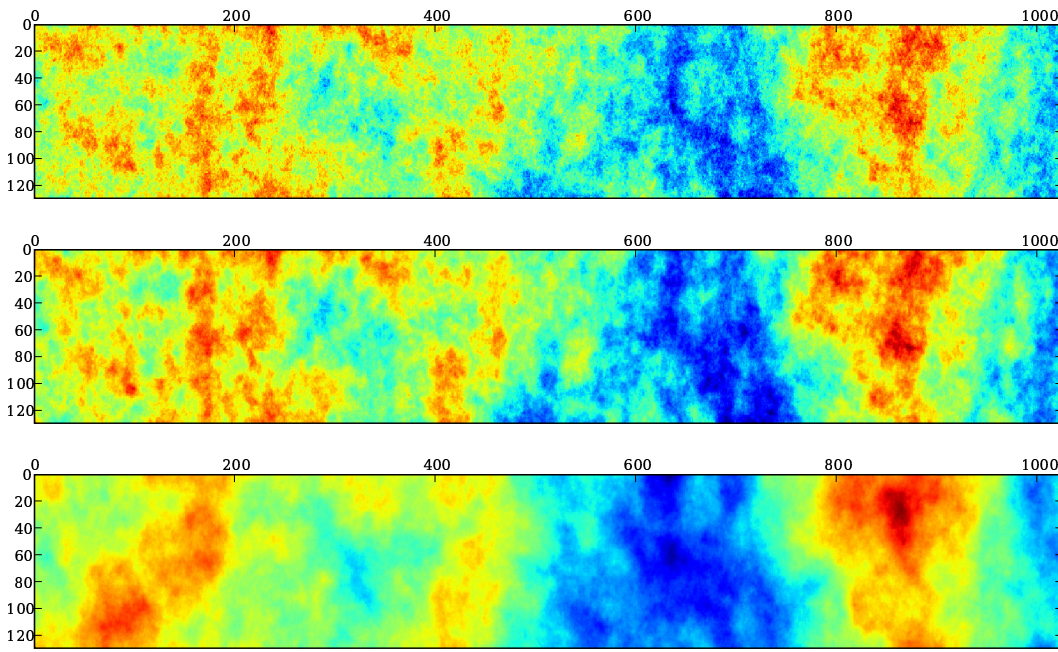


**Figure 1.** Simulation of three dimensional turbulence on a  $1025 \times 129 \times 129$  grid (i.e., a sub-section of the grid used for the simulations below). Top: a single horizontal slice  $k = 0$ , where  $k$  is the vertical index of the grid; Middle: sum of slices  $0 < k < 10$ ; Bottom: sum of slices  $0 < k < 100$ .

each element of volume are proportional to  $q$  and that this emission is always fully optically thin so that radiative transfer effects are not important. Observed radiometer brightness temperatures and the field  $q$  are then related in a linear way.

Assumption (i) above is likely to be good in the conditions under investigation although the factor of proportionality depends slightly on the temperature. Assumption (ii) is dependent on the frequency at which the WVRs observe, the absolute quantity of water, temperature, etc. In general it will not hold, but with WVR designs that have several channels that sample different parts of the water vapour emission line (the ALMA design has four channels, Hills et al. 2001), it is usually possible to derive an equivalent quantity that is linear in  $q$ .

## 2.1 Generating the turbulent field

We wish to generate statical realisations of a turbulent field  $q(x, y, z)$ , namely a field that obeys the property:

$$\left\langle [q(\mathbf{r}') - q(\mathbf{r}' + \mathbf{r})]^2 \right\rangle = D_q(|\mathbf{r}|) = D_q(r) = 6.88 \left( \frac{r}{r_0} \right)^\xi. \quad (1)$$

The factor of 6.88 on the right hand side is conventional so that  $r_0$  is then the Fried parameter (Lane et al. 1992). For approaches which use two-dimensional turbulent screen the question arises of the correct exponent  $\xi$  in the defining structure function  $D_q$ : when the geometry of the telescope is much smaller than the thickness of the turbulent layer a coefficient of  $\xi = 5/3$  is appropriate while in the opposite limit  $\xi = 2/3$  is more appropriate. Here we are generating three-dimensional turbulence so the expected exponent is  $\xi = 2/3$  – the observed steepening of the structure function is naturally reproduced in our case by averaging over volumes of the turbulent field (see Figure 1).

The algorithm we actually use to compute the statistical realisations of  $q$  is a generalisation to three dimensions of the algorithm

of Lane et al. (1992). It has been developed by us for this application and can efficiently simulate fields with more than  $10^9$  volume elements.

Since we wish to quantify the effect of differences between the astronomical and WVR beams, the resolution of the realised fields must be good enough to resolve this; for the results presented here we use  $1 \text{ m}^3$  in all simulations. Most of the simulations (except that shown in Figure 1) have been carried out for fields with dimensions of the order of  $4097 \times 257 \times 513$  resolution elements.

## 2.2 Refractive index and the received astronomical signal

This section summarises the theory which relates fluctuations in the refractive index (i.e.,  $q$  in our case) to the received astronomical signal at each antenna.

The fundamental property that we use is that the signal received may be computed as the surface integral of the product of the incoming field and the antenna voltage response over any plane (or any other infinite surface) between the source and the antenna. Working in Cartesian coordinates  $\{x, y, z\}$  such that  $z$  is the direction from the antenna toward the source, we write the incoming wavefront as the complex electric field  $E(x, y, z)$  and the antenna voltage response pattern as  $A(x, y, z)$ . The above property means that the received signal is:

$$V = \iint dx dy A(x, y, z) E(x, y, z) \quad (2)$$

evaluated over any plane  $z = h$ . Clearly the signal does not depend on the plane over which the integral is evaluated and so  $A$  and  $E$  must vary with height above the telescope in such a way that  $V$  does not change.

When the medium in which radiation propagates is homogeneous, the problem of calculating  $V$  is easily solved using Fourier transforms, i.e., the angular response functions is simply the Fourier transform of the aperture plane response function:

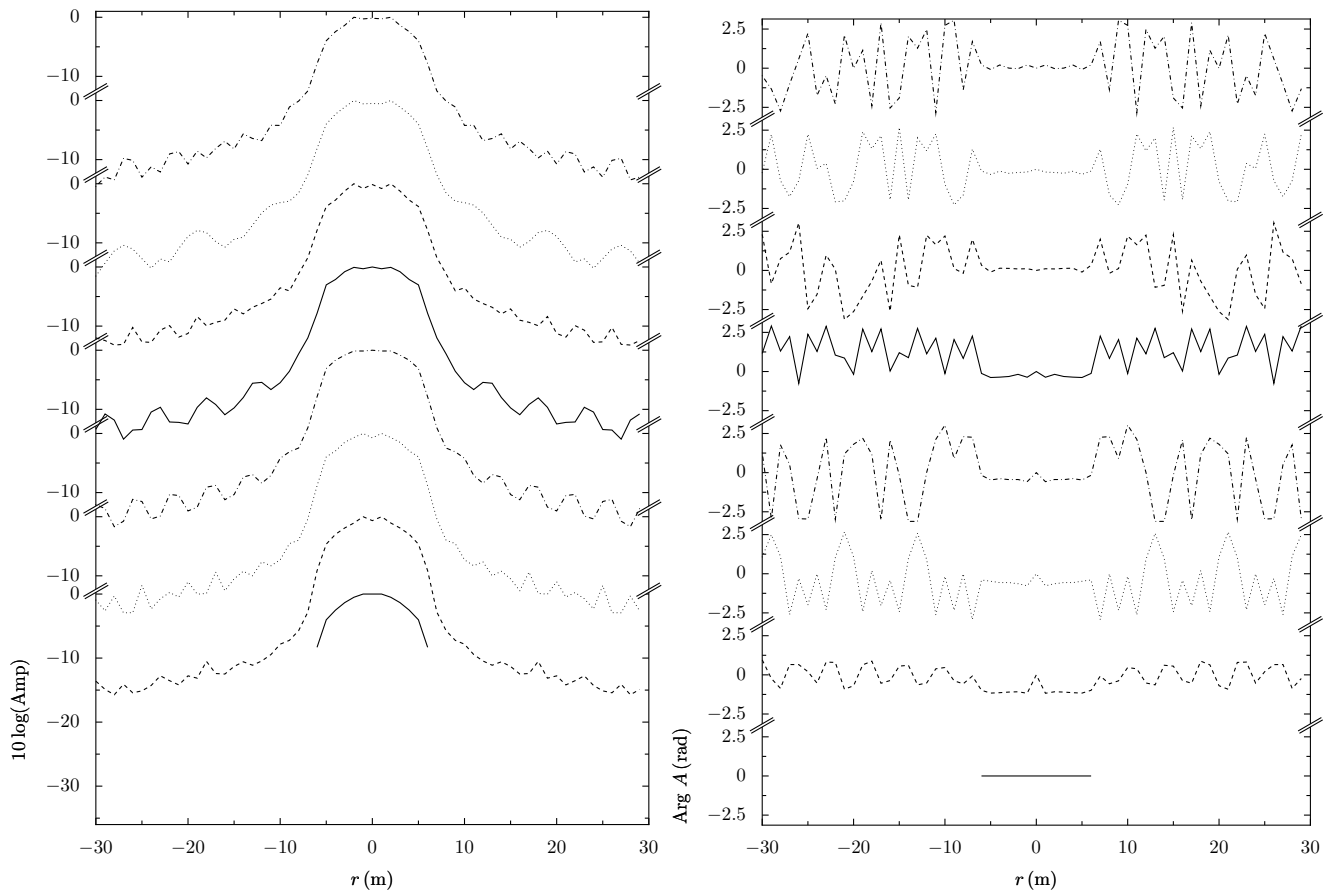


**Figure 2.** Horizontal cuts of the amplitude (left) and phase (right) of the astronomical beam for eight distances from the antenna starting at the aperture plane (bottom) and increasing in 500 m steps to 3500 m (top).

$$A(u, v) = \mathcal{F} \mathcal{T} [A(x, y; z = 0)]. \quad (3)$$

This makes it possible to calculate easily how a single antenna will respond to a source as a function of its position. Alternatively, the surface integral of Equation 2 may also be calculated at the aperture of the antenna (that is,  $z = 0$ ), which is convenient since  $A(x, y, z = 0)$  is easy to compute. In the case of a point source and a homogeneous atmosphere, the incoming radiation at  $z = 0$  will be a plane wave and so the integral is easy to compute.

We note two straightforward points. First, when calculating the surface integral at  $z = 0$  an aperture of finite size will still of course have a finite angular response. This can be appreciated by considering an incoming plane wave at an angle  $u$  from the vertical: this will cause a range of phases across any finite-sized apertures leading to a decrease in the final complex sum when calculating  $V$ .

Second, although conventionally the integral of Equation (2) is done at  $z = 0$  or  $z = \infty$ , it may be done at any  $z$ . If the incoming waves are planar and the medium through which they propagate is homogeneous, they can be trivially computed at any  $z$ . Similarly, if the medium of propagation is homogeneous, the antenna voltage response  $A(x, y, z)$  may be quite easily approximately computed from the aperture-plane response  $A(x, y; z = 0)$  using the Fresnel integral.

The general case of propagation through an in-homogeneous medium is more complicated. If smallest scale structure in the medium is at the length scales of about  $\Delta$  and the wavelength of radiation is  $\lambda$  then diffraction due to the medium becomes important a distance approximately  $\Delta^2/\lambda$  into the medium. In the case

of the present study  $\Delta \approx 1$  m since the resolution of our statistical realisations of turbulence is 1 meter and  $\lambda \approx 1$  mm so diffraction due to inhomogeneities may become significant at around 1 km.

Since the thicknesses of turbulent layers we consider in this note are all smaller than this length, we can apply the following approximation. We flatten the turbulent layer in the required direction (that is, taking into account the offset the beams) and consider that it as a thin screen. That is, we compute:

$$q'(x, y; \theta, \xi) = \int dr q(r_x(z), r_y(z), z) = \quad (4)$$

$$\int dz q(x + z \sin(\theta) \sin(\xi), y + z \sin(\theta) \cos(\xi), z), \quad (5)$$

where the angles  $\theta$  and  $\xi$  define the offset of the beam with respect to the vertical such that  $\xi = 0$  is an offset in the direction of the baseline and  $\xi = \pi/2$  is an offset in the windward direction.

It is this computation of  $q'$  from  $q$  which produces the correct steepening of the structure function without supplying the exponent  $\xi$  but rather just the physical thickness of the turbulent layer in the atmosphere.

The integral of Equation 2 is then very conveniently performed at the height of the turbulent layer without the need to compute the diffraction due to atmospheric fluctuations. If we are considering a single source exactly on the antenna axis then we can assume  $E(x, y; z = h) = 1$  and thus:

$$V[q'] = \iint dx dy \cdot A(x, y, z = h) \cdot e^{iC_w q'(x, y)} \quad (6)$$

where  $C_w$  is the conversion factor between phase and water content. The argument of  $V[q']/V[0]$  is the phase shift introduced by atmospheric turbulence  $q$  and the magnitude of  $V[q']/V[0]$  corresponds to the decrease amplitude of received signal due to the turbulence, i.e., ‘radio-seeing’.

### 2.3 The signal measured by the WVRs

Computing the signal received by the WVRs is relatively simple because the emission from the water molecules will not be coherent and because we have assumed that radiation is propagating in a perfectly optically thin way. The signal received by the WVRs,  $W[q]$ , could therefore be computed by integrating the water-vapour distribution  $q$  weighted by the antenna power-response pattern  $P(x, y, z) = |A(x, y, z)|^2$ . For consistency with Equation (6), we however also calculate the power received by the radiometers from ‘flattened’ water-vapour distribution  $q'$ :

$$W[q'] = \int \int dx dy \cdot P(x, y, z = h) \cdot q'(x, y). \quad (7)$$

### 2.4 Computing the antenna response patterns

We assume that the astronomical beam has a -12 dB edge taper and that the WVR beam has -18 dB edge taper. Both beams are modelled as Gaussian with the blockage by the secondary mirror (but not the supports) taken into account (we also of course take into account the truncation of beams by the size of the primary reflector). The antenna response at an altitude  $h$  is computed using Fresnel integrals, which we approximate by adding quadratic phases to the aperture-plane field distribution and using the straightforward Fast-Fourier Transform (FFT).

For the astronomical beam both the phase and the amplitude of the antenna response are calculated and they are shown as functions of altitude in Figure 2. For the WVR beam only the power response is relevant and it is shown in Figure 3.

### 2.5 Time series of phase and WVR measurements

The geometry which we use to generate the simulated time series is as follows. We assume that the two antennas are observing at the zenith and are separated by a distance  $b$  in the  $y$  direction and calculate the differences between the received phases (of the astronomical signal), which we will write  $\phi$ , and powers from the WVRs, which we denote by  $W$ . In order to generate the time series we sequentially translate this baseline in the  $x$ -direction. We will assume that the sampling is done at 1 s so the distance translated is simply  $v/1$  s where  $v$  is the wind-speed, i.e., the speed with which an apparently frozen phase screen is moving across the telescope. The geometry is shown in Figures 4 and 5. When the antennas are not observing toward the zenith, the quantities  $h$  and  $w$  should be scaled by the secant of the zenith angle to account for the longer apparent distance to the turbulent layer and the greater apparent thickness of the turbulent layer respectively.

This procedure produces astronomical phase differences  $\phi_i$  and water vapour differences  $W_i$ . We assume that the best estimate of phases from water vapour measurements,  $\hat{\phi}$ , is the best-fit linear scaling, i.e.,  $\hat{\phi}_i = cW_i$ , where  $c$  is a constant. The error in our estimate of phase fluctuation is  $\phi - \hat{\phi}$  and we define the overall fractional error as:

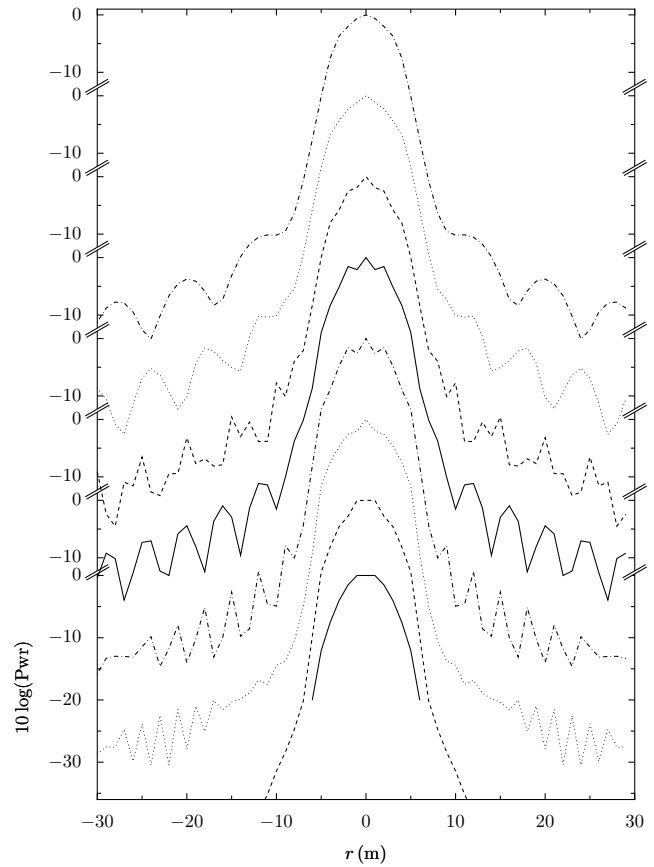


**Figure 3.** Horizontal cuts of the power response of the water-vapour radiometer beam for the same eight distances as shown in Figure 2.

$$(\delta\sigma)^2 = \frac{\langle (\phi - \hat{\phi})^2 \rangle - \langle \phi - \hat{\phi} \rangle^2}{\langle \phi^2 \rangle - \langle \phi \rangle^2}. \quad (8)$$

In order to reduce the effect of statistical variance when computing  $\delta\sigma$  we generate ten statistical realisations of Kolmogorov turbulence and quote  $\delta\sigma$  as the mean of the values computed for each turbulence realisation.

## 3 RESULTS

For the results presented in this section the following parameter ranges were considered.

Turbulent layer thicknesses ( $w$ ) in the range from 1 to 500 m have been used. The smallest values  $w$  are unlikely to be physically relevant but we include them for comparison with thin-screen approximations. The results for different thicknesses are shown by different line styles.

Simulations have been made for three heights of the turbulent layer:  $h = 250$  m,  $h = 750$  m and  $h = 1250$  m. Measurements using two site testing interferometers at the Chajnantor site by Robson et al. (2001) indicate that most of turbulence is below 500 m while Beaupuits et al. (2005) show with radiometric tests that the turbulent layer is likely to be around  $h \approx 700$  m. Hence, the range of heights we have used in our simulations brackets the likely heights of the turbulent layer at the ALMA site.

Three values of length of the baseline between the antennas have been used:  $b = 64$  m,  $b = 128$  m and  $b = 256$  m. We have

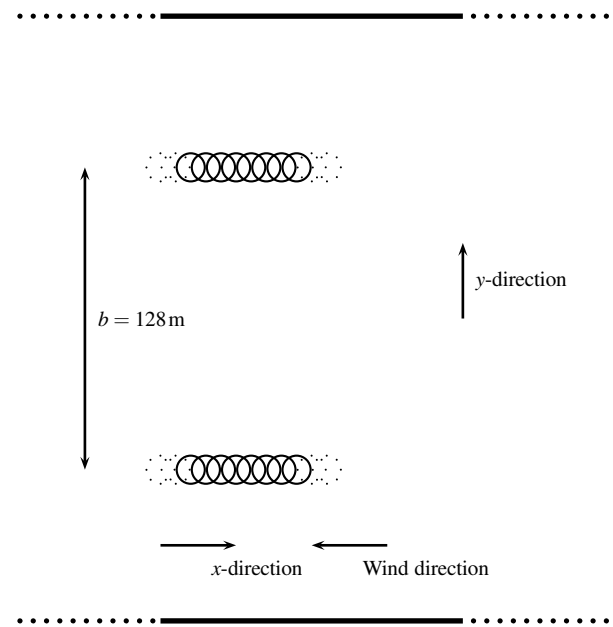


Figure 4. Illustration of simulation of time series of fluctuations

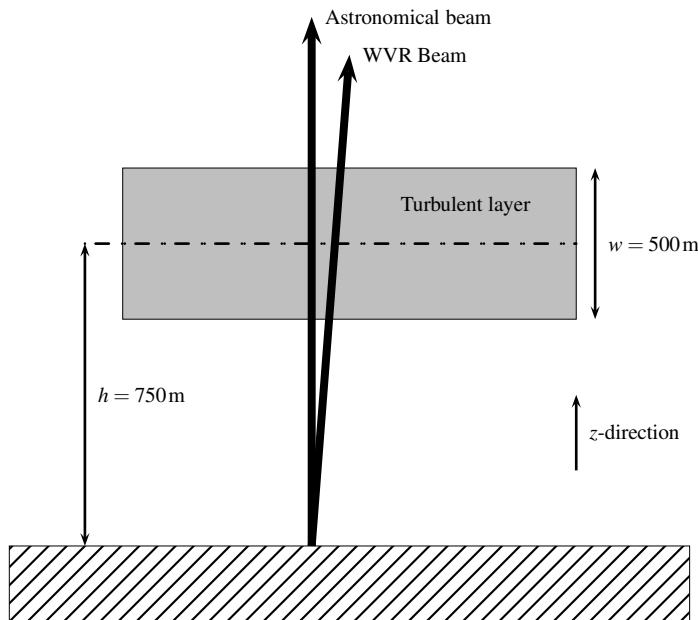


Figure 5. Illustration of the geometry of the turbulent layer and the astronomical and WVR beams.

not considered longer baselines because it would be considerably more complex to carry out simulations of both the sufficient size to accommodate these baselines and the sufficient resolution to resolve the effects of the differences between astronomical and WVR beams. Furthermore, the relative size of error due to beam-mismatch is less significant at longer baselines.

All simulations presented here have been carried out under the assumption that astronomical observing is being carried out  $\lambda = 1$  mm. We have of course assumed that the radiometers are observing close to water vapour line they are measuring, i.e., 183 GHz.

It has been assumed that the displacement between the astronomical and the WVR beams is in the direction perpendicular to wind. We note that if the displacement is in the direction of the wind it may, in principle, be possible to reduce the error due this displacement by shifting the WVR measurements in time. This can not be done in the present geometry.

The range of displacement angles ( $\delta\theta$ ) considered is from zero up to 30 arc-minutes. The displacements of astronomical from the WVR beams in the present design of ALMA 12-m antenna and front-ends are shown in Table 1 and they range from 3.58 to 9.13 arc-minutes. Hence, the range of displacements considered in the figure is larger than the maximum that will occur in the case of ALMA, but. It is nevertheless plotted to better show the trends and also as an aid for those considering designs of similar antennas.

A sample of the simulated phase fluctuations in the astronomical signal, the simulate signal received by the radiometers and the difference for the when the beams are perfectly coincident is shown in Figure 6. Figure 7 shows how the root-mean-square of fluctuations varies with the baseline length for a number of baseline thicknesses.

The key results are shown in Figures 8 and 9. The both show fractional error in fluctuations as seen by the astronomical signal and the radiometers as the function of beam displacement. Figure 8 shows this variation three heights of the turbulent layer while Figure 9 shows the variation for three baseline lengths.

The final result is shown in Figure 10, which illustrates the effect of the tapers of the astronomical and radiometer beams by repeating the simulation for radiometers with -5 dB and -30 dB tapers. Because the radiometer measures incoherent radiation from water, the -5 dB taper corresponds closely to the -12 dB taper of the astronomical receivers. As a result, it can be seen that the discrepancy between phase fluctuations and radiometer outputs is very small for small beam displacements. With a -30dB edge taper, the radiometer beam in the near field is a rather narrow cylinder and therefore samples the water only close to the centre of the astronomical beam. The resulting discrepancy between measurement by the radiometer and the phase fluctuation of the astronomical signal is shown in the bottom plot of Figure 10.

#### 4 DISCUSSION AND CONCLUSIONS

Due to design constraints, the water vapour radiometers for ALMA will not sample parts of the atmosphere which are geometrically exactly the same as those causing the fluctuations in the phase of the received astronomical signal. This effect alone will cause some error in estimates derived from the WVR measurements that are used to correct for the atmospheric phase fluctuation, and the results shown in the previous section quantify the size of these errors.

The specification for atmospheric phase correction for the ALMA project require that the residual (i.e., after correction) root-mean-square fluctuations are equal to or less than  $10\mu\text{m}(1 + \frac{c}{1\text{mm}})$

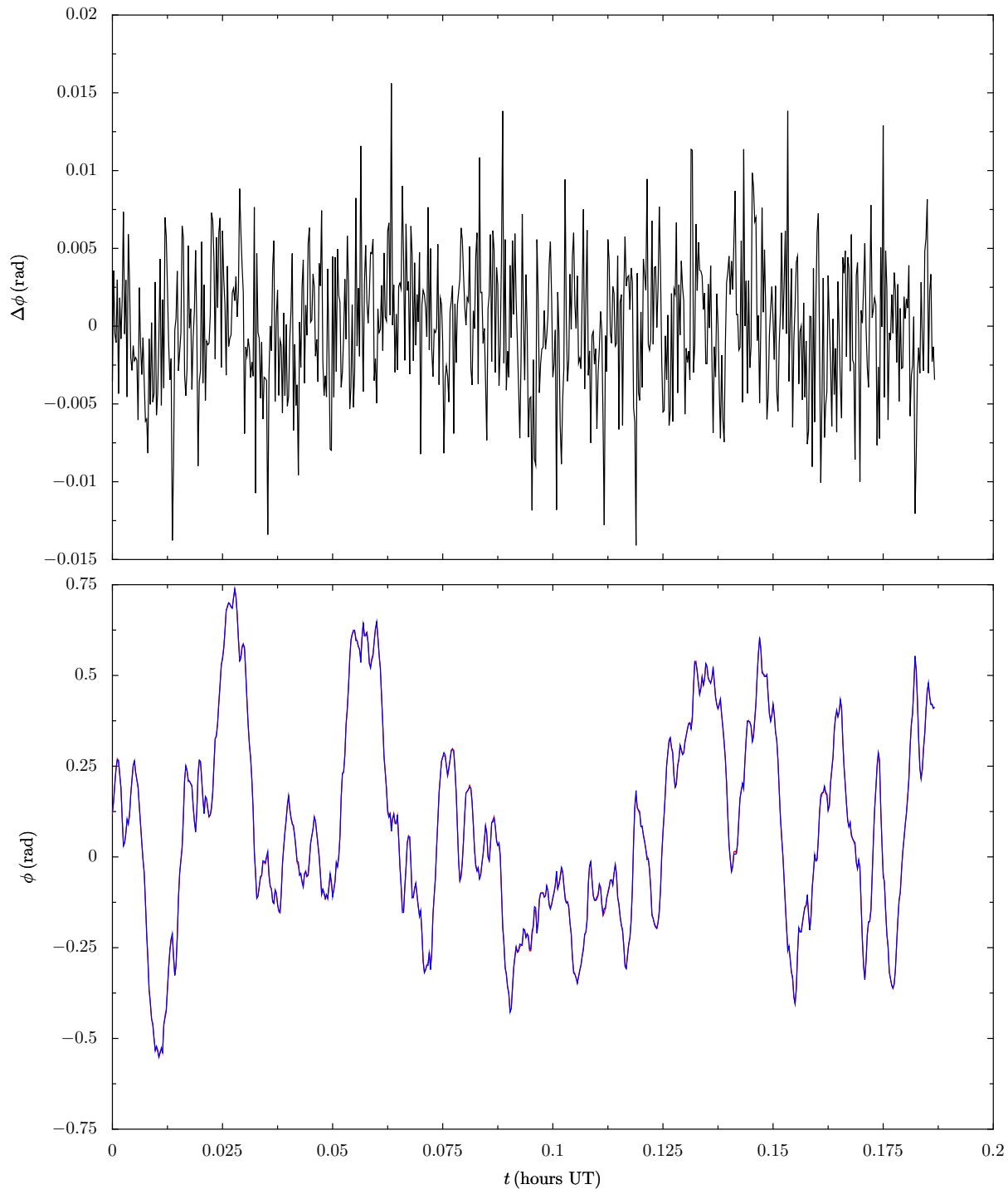


**Figure 6.** Simulated phase fluctuations (bottom panel) and the error in phase fluctuations inferred from the simulated radiometer data (top panel). The simulation was carried out for a 128 m long baseline, a 500 m thick turbulence layer and a wind speed of  $6 \text{ m s}^{-1}$ . The astronomical and WVR beam shapes used were as shown in Figures 2 and 3 and the beams were assumed to be exactly aligned.

per antenna plus two per-cent of fluctuation on any one baseline. Here  $c$  is the precipitable water vapour column. As the error due to geometric mismatch discussed here is proportional to the magnitude of the fluctuations, it should ideally be accounted for in the proportional part of the error budget.

Measurements of un-corrected atmospherically-induced phase fluctuations at the ALMA site (reviewed by Evans et al. 2003) show

that in good night time conditions, the fluctuations on a 300 m long baseline are around  $100 \mu\text{m}$ , while in poor day-time conditions they may be as high as  $900 \mu\text{m}$ . Extrapolating from Figure 7, this corresponds on a 128 m baseline to approximately 60 and  $600 \mu\text{m}$ . Hence under good night time conditions a proportional error in phase correction of around two-percent will still be small compared to the specification for the additive error (minimum  $10 \mu\text{m}$  per an-

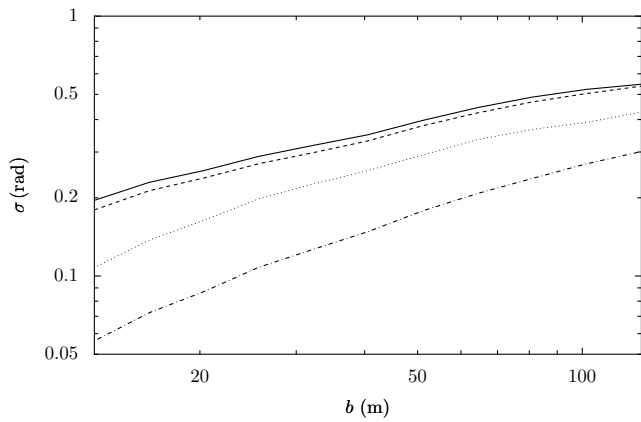


**Figure 7.** Root-mean-square of phase fluctuations of the received signal as function of baseline length for four thicknesses of the turbulent layer: thin-screen (solid line), 10 m, 100 m and 500 m (dot-dash-dot line).

tenna or  $14 \mu\text{m}$  per baseline). Under conditions when uncorrected fluctuations are strong, a proportional error of two-percent, will however be comparable to the additive error. Although the magnitude of uncorrected fluctuations increases on long baselines, as discussed below, the relative importance of the errors studied in this memo decreases.

The typical case we consider in this note is a baseline between antennas of length 128 m and a turbulent layer which at a height 750 m (this case is shown in Figures 8, 9 and 10). The physical thickness of the turbulence layer at Chajnator is likely to be between 100 and 500 m, i.e., between the bottom two lines in the plots of the previous section. As can be seen from the plots, the fractional error due to the geometric mismatch is in the range between one and two per-cent when the beams are exactly aligned and the increase with angle of mis-alignment becomes significant when the displacement is about 5 arc-minutes. Therefore in the case the ALMA, the geometric mismatch is of the order of the proportional part of the error budget and in order to meet the specifications it will be necessary to minimise other effects which introduce errors that are primarily proportional to the magnitude of fluctuations.

The differences between the three plots in Figure 8 show the significance of the height of the turbulent layer. If the WVR and astronomical beams are exactly aligned the height is only of small importance (arising due to diffraction of the beams). As expected, the error due to misalignment increases with increasing height of the turbulent layer: if the layer is at 1250 m then the fractional error due to mis-alignment becomes significant at an mis-alignment angle of around 2.5 arc-minutes.

The three plots in Figure 9 show how the calculated limits on performance vary with the length of the baseline between the antennas. They show that at longer baselines the effect of geometric mismatch becomes relatively less significant. The final Figure 10 illustrates the significance of the taper of the radiometer beam. It is easier to minimise the spillover of the radiometers with a large taper, but as is illustrated in this figure, this is at a cost of limitations on the accuracy with which the fluctuations can be measured. The -18 dB maximum taper specified by ALMA is a compromise between these trade-offs. The top panel of Figure 10 shows that if the taper were as low as -5 dB, this would make the error with exactly aligned beams insignificant. On the other hand, a large taper of -30 dB would significantly increase the error due to geometric mis-match.

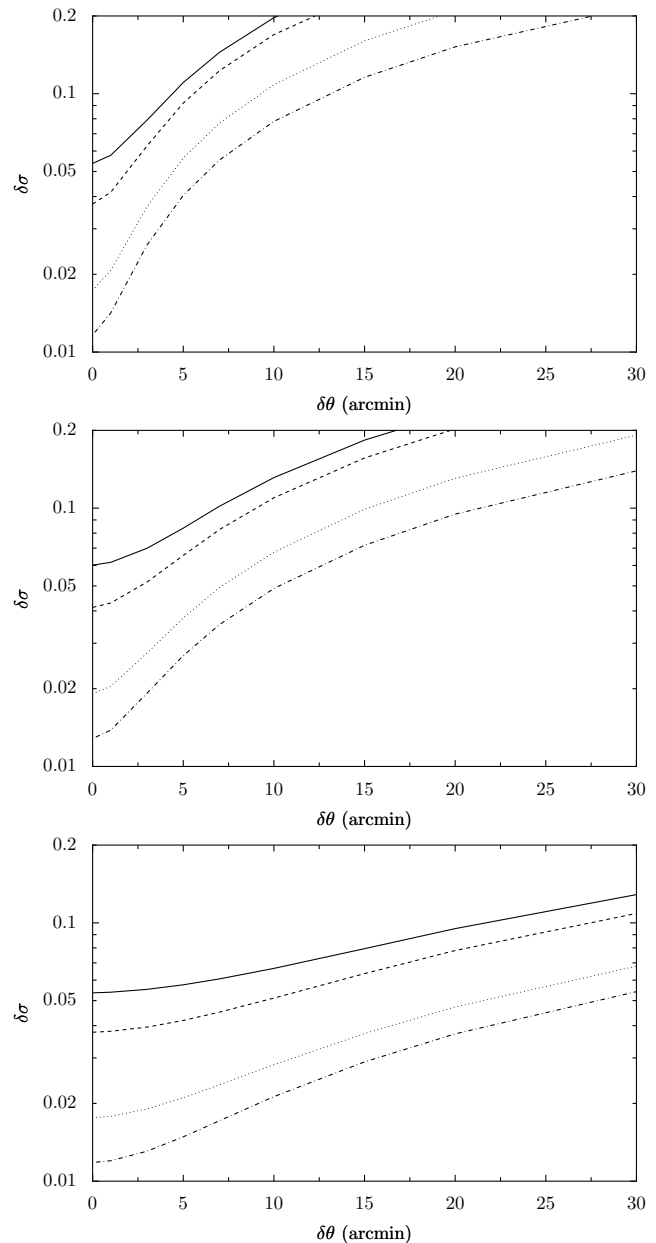


**Figure 8.** Fractional error in estimated phase fluctuations as function of the beam offset. Bottom plot is for a turbulent layer at a height of 250 m, middle for height of 750 m and top for height of 1250 m. For each layer height, the error for four layer thickness have been calculated: thin-screen (solid line), 10 m thick layer (dashed line), 100 m thick layer (dotted line) and 500 m thick layer (dash-dot-dash line).

Within the context of ALMA these results may be summarised as follows. It has been possible to minimise the effect of the displacement of the radiometer and astronomical beams by placing the highest frequency receiver bands closest to the pick-off mirror of the radiometer. These displacements are shown in Table 1.

Because of this, for the highest frequency bands, the angular displacement of the astronomical and WVR beams contributes about the same to the phase correction error budget as the other effects studied in this memo, namely the error due to the incoherent nature of the water-vapour radiometer measurement as opposed to the coherent detection of the astronomical signal and the differ-

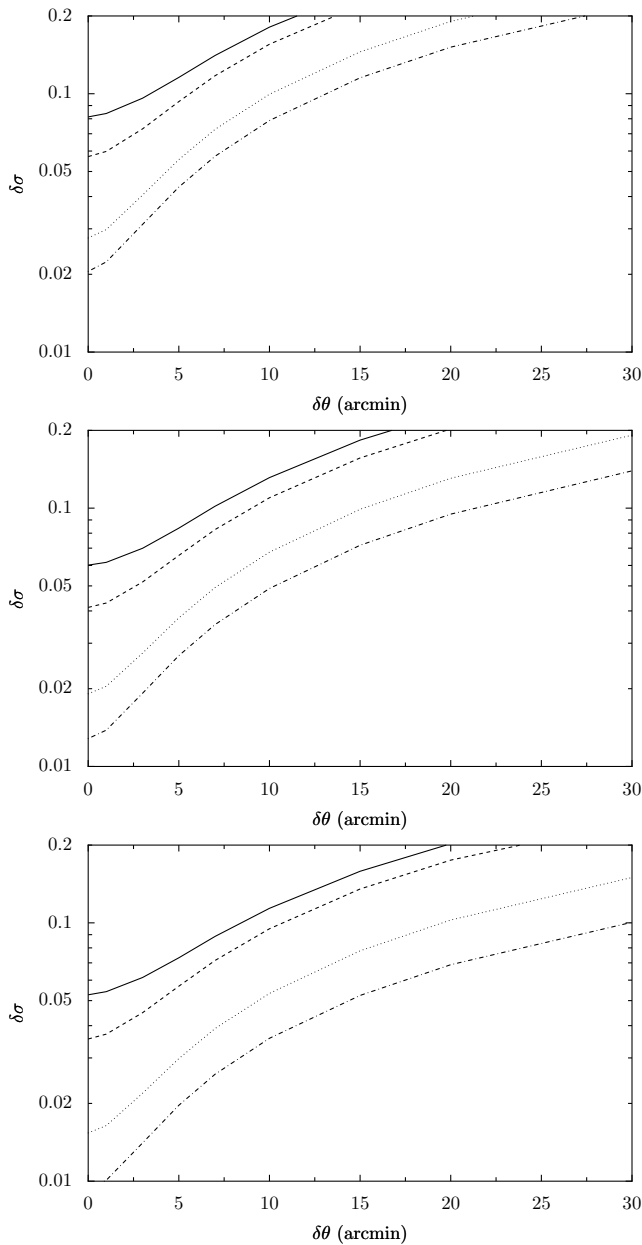


**Figure 9.** Fractional error in estimated phase fluctuations as function of beam offset, as in Figure 8, but showing the significance of the baseline length. The turbulent layer is assumed to be centred at a height of 750 m and errors have been calculated for four thicknesses: thin-screen (solid line), 10 m (dashed line), 100 m (dotted line) and 500 m (dash-dot-dash line). The three panels show the results for three baseline lengths (top to bottom): 64, 128 and 256 m.

ent edge tapers of the two receivers. (In practice of course effects not considered in this note, such as the radiometer measurement error and the uncertainty in atmospheric modelling, will also be important.) Unless the turbulence is concentrated at very low heights in the atmosphere, the larger angular displacement of the lower-frequency receivers will place further significant limits on the possible performance of the radiometers, as shown in Figure 8.

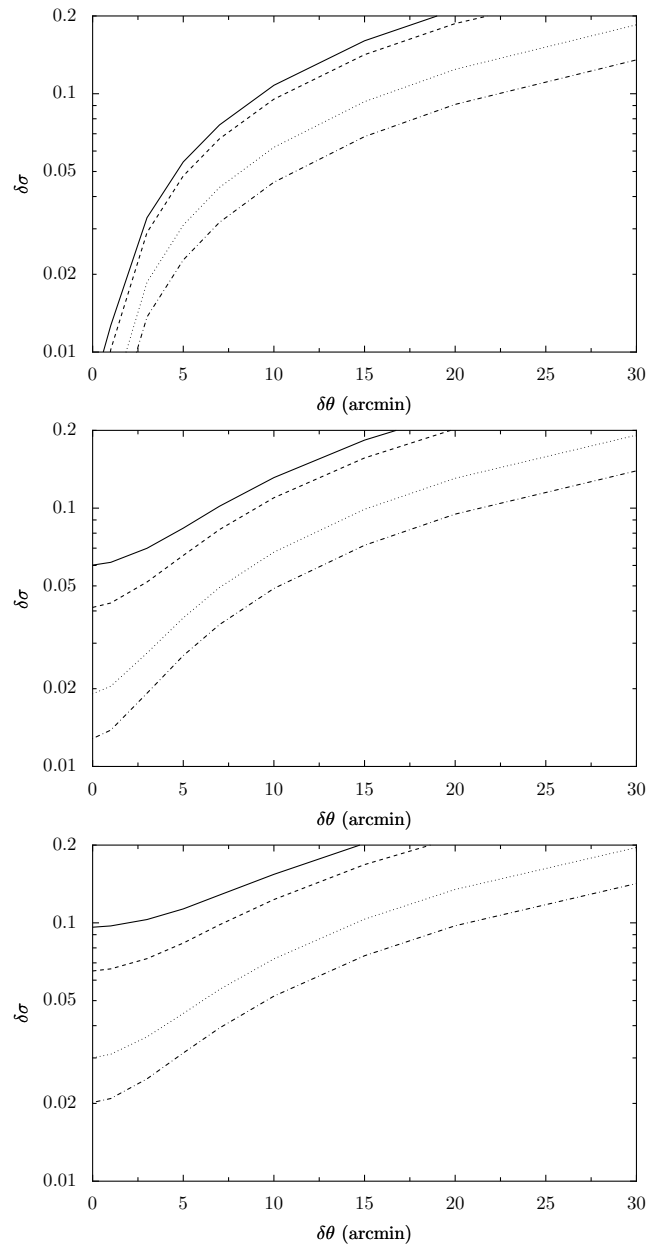


**Figure 10.** Fractional error as function of beam offset for three tapers of the WVR beam. The middle plot is has -18dB taper as previously; top plot is for -5dB taper; bottom plot is for -30 dB taper. Baseline length is 128 m height of turbulent layer 750 m as before.

#### ACKNOWLEDGEMENTS

We wish to thank Darrel Emerson for a careful reading of the manuscript and helpful comments.

#### REFERENCES

- Asaki A., Saito M., Kawabe R., Morita K., Tamura Y., Vila-Vilaro B., 2005, ALMA Memo Series 535, Simulation Series of a Phase Calibration Scheme with Water Vapor Radiometers for the Atacama Compact Array. The ALMA Project  
 Beaupuits J. P. P., Rivera R. C., Nyman L.-Å., 2005, ALMA Memo Series 542, Height and Velocity of the Turbulence Layer

Band	Frequency range (GHz)	$\delta\theta$ (arc-minutes)
1	31.3-45	9.13
2	67-90	9.13
3	84-116	6.77
4	125-163	7.05
5	163-211	8.77
6	211-275	8.77
7	275-373	3.58
8	385-500	3.58
9	602-720	3.58
10	787-950	3.58

**Table 1.** Displacement between beams of astronomical ALMA receivers and the beam of the water-vapour radiometer.

at Chajnantor Estimated From Radiometric Measurements. The ALMA Project  
 Evans N., Richer J. S., Sakamoto S., Wilson C., Mardones D., Radford S., Cull S., Lucas R., 2003, ALMA Memo Series 471, Site Properties and Stringency. The ALMA Project  
 Gibb A. G., Harris A. I., 2000, ALMA Memo Series 330, The overlap of the astronomical and WVR beams. The ALMA Project  
 Hills R. E., Gibson H., Richer J. S., Smith H., Belitsky V., Booth R., Urbain D., 2001, ALMA Memo Series 352, Design and Development of 183GHz Water Vapour Radiometers. The ALMA Project  
 Lane R. G., Glindemann A., Dainty J. C., 1992, Waves in Random Media, 2, 209  
 Robson Y., Hills R. E., Richer J. S., Delgado G., Nyman L.-Å., Otarola A., Radford S., 2001, ALMA Memo Series 345, Phase Fluctuation at the ALMA Site and the Height of the Turbulent Layer. The ALMA Project